WAVELET ANALYSIS OF THE AUGUST 17, 2022 GEOMAGNETIC STORM

ASIMOPOLOS Laurenţiu, ASIMOPOLOS Natalia-Silvia, ASIMOPOLOS Adrian-Aristide, BALEA-ROMAN Bogdan-Valeriu-Constantin

Abstract. The purpose of this work is to multi-spectrally analyse the strongest geomagnetic storm of the year 2022. According to specialized international websites, this storm occurred on August 17, 2022. We used the triaxial and total geomagnetic field data, monitored with a sampling rate of one minute, in 6 planetary geomagnetic observatories. The geomagnetic observatories from the INTERMAGNET network that we used in these analyses are located at very different latitudes and longitudes on the Earth's surface. Among these, we exemplified the complex wavelet and coherence analyses between the Surlari (Romania) and Ebre (Spain) observatories. We also used the physical parameters related to this geomagnetic storm, from the available data. The Fourier transform gives us information only in terms of frequency and amplitude, but it cannot highlight which of the harmonic components are present at a given moment in a series of geomagnetic data. Wavelet analysis gives us information in the form of a three-dimensional graph (time, frequency, amplitude). In the two-dimensional plane, time and frequency are present and the amplitude is coded by colour intensity levels. In addition, wavelet coherence is a very useful procedure for non-stationary signals, such as geomagnetic data. Based on the comparisons made between the analysed and exemplified geomagnetic data, we can observe a very good correlation between them.

Keywords: Geomagnetic Storm, Planetary Geomagnetic Indices, Wavelet Analyses, Wavelet Coherence.

Rezumat. Analiza wavelet a furtunii geomagnetice din 17 august 2022. Scopul acestei lucrări este de a analiza multi-spectral cea mai puternică furtună geomagnetică din anul 2022. Conform site-urilor internaționale specializate, această furtună a avut loc în 17 august 2022. Am folosit datele de câmp geomagnetic triaxial și total, monitorizate cu rata de eșantionare de un minut, în 6 observatoare geomagnetice planetare. Observatoarele geomagnetice din rețeaua INTERMAGNET pe care le-am folosit în aceste analize sunt dispuse la latitudini și longitudini foarte diferite pe suprafața Pamântului. Dintre acestea, am exemplificat analizele complexe wavelet și de coerență dintre observatoarele Surlari (România) si Ebre (Spania). De asemenea, am folosit și parametrii fizici legați de această furtună geomagnetică, din datele disponibile. Transformata Fourier ne dă informații doar în planul frecvență și amplitudine, dar nu poate evidenția care dintre componentele armonice sunt prezente la un moment dat într-o serie de date geomagnetice. Analiza wavelet ne oferă informații sub forma unui grafic tridimensional (timp, frecvență, amplitudine). În planul bidimensional sunt prezente timpul și frecvența, iar amplitudinea este codificată prin niveluri de intensitate a culorii. In plus, coerența wavelet este un procedeu foarte folositor pentru semnalele nestaționare, așa cum sunt datele geomagnetice. Din comparațiile efectuate asupra datelor geomagnetice analizate și exemplificate putem observa o corelație foarte bună între acestea.

Cuvinte cheie: furtuna geomagnetică, indici geomagnetici planetari, analiza wavelet, coerența wavelet.

INTRODUCTION

Space weather is determined by four main components: solar flares consisting of X-ray solar flashes, coronal mass ejections (CME's), high speed solar wind, and solar energetic particles, and refers to the effects that the Sun has on Earth and the planets of the solar system. A Coronal Mass Ejection (CME) is a massive cloud of hydrogen ions that is ejected from the surface of the Sun when the stored energy is suddenly released. The CME produces a cloud of high energy particles traveling at very high speeds (500-2000 km per second). When a CME is ejected towards Earth it reaches us within around two days. The impact of the CME on the Earth causes a disturbance to the Earth's magnetic field. The solar wind is a stream of charged particles ejected from the upper atmosphere of the Sun. It mostly consists of electrons and protons and varies in temperature and speed over time (CAMPBELL, 2003).

Geomagnetic storms are caused by the interaction of the solar wind with Earth's magnetic field. When the solar wind encounters the Earth's magnetic field, it can cause the magnetic field lines to stretch and compress. This can cause energy to be transferred from the solar wind into Earth's magnetosphere and ionosphere, which can lead to geomagnetic storms (ASIMOPOLOS et al., 2012).

A geomagnetic storm is defined by changes in the Dst (disturbance – storm time) index. The Dst index estimates the globally averaged change of the horizontal component of the Earth's magnetic field at the magnetic equator based on measurements from four geomagnetic observatories.

According to https://www.spaceweatherlive.com/ (in link: the top 50 geomagnetic storms of 2022), details can be found about the strongest geomagnetic storm in 2022 from August 17. Also, can be find an overview of the strongest geomagnetic storms of 2022 together with links to more information in their archive (e.g., the Kp-values on https://www.gfz-potsdam.de/en/, finalized Kp-values from the GFZ in Potsdam, Germany (https://www.gfz-potsdam.de/en/).

The Geomagnetic Storm Scale indicates the severity of geomagnetic storms. It is denoted by a G followed by a number from 1 to 5, with G1 being a minor event, and G5 being an extreme event.

The scale uses the planetary K-Index, Kp as its physical measure, the scale levels are between 1 to 9.

The event of August 17 that I studied falls under the strong geomagnetic storms, with a maximum Kp of 7 that can have the following consequences:

Power systems: voltage corrections may be required, false alarms triggered on some protection devices.

Also, intermittent satellite navigation and low-frequency radio navigation problems may occur, HF radio may be intermittent, and aurora can be seen at 50° geomagnetic latitude.

There are several ways to analyse geomagnetic storms. One way is to use the World Magnetic Model (WMM) which produces data that is reliable five years after the epoch of the model.

Another way is to study the variation of geomagnetic storm duration with intensity. Geomagnetic storms are one of the main factors of Space Weather. The storms significantly influence on the interconnected dynamical system of the Earth magnetosphere-atmosphere-ionosphere and result in deteriorated operation of global navigation satellite systems (GNSS), radar systems, communication systems and others critical infrastructures (ASIMOPOLOS N. S. & ASIMOPOLOS L., 2018).

METHODOLOGIES

Geomagnetic signals, recorded in observatories with different sampling rates, are the convolution product of the atomic stationary signal mono-frequential of different amplitudes associated to phenomena with a very broad band of periodicities and nondeterministic signals associated with geomagnetic disturbances and non-periodic phenomena.

Among analysis processes used for discrete series of geomagnetic data, time-frequency analyses or wavelet analysis, the advantage of wavelet transformations versus the Fourier transform is the possibility to analyse discrete data sets that have some gaps or irregular variations, as the geomagnetic data (BOX et al., 2016).

Continuous Wavelet Transform (CWT) can be used to analyse how the frequency content of a geomagnetic signal changes over time. We can perform adaptive time-frequency analysis using nonstationary Gabor frames (GRINSTED et al., 2004; MARAUN et al., 2003). For two signals, wavelet coherence reveals common time-varying patterns. Also, we can perform data-adaptive time-frequency analysis of nonlinear and nonstationary processes (https://www.mathworks.com/).

The wavelet cross-spectrum is a measure of the distribution of power of two signals. The wavelet cross spectrum of two time series, x and y, is:

$$C_{xy}(a,b) = S(C_x^*(a,b)C_y(a,b))$$

where: Cx(a,b) and Cy(a,b) denote the continuous wavelet transforms of x and y at scales a and positions b. The superscript * is the complex conjugate, and S is a smoothing operator in time and scale.

For real-valued time series, the wavelet cross-spectrum is real-valued if you use a real-valued analysing wavelet, and complex-valued if we use a complex-valued analysing wavelet.

Wavelet coherence is a measure of the correlation between two signals.

The wavelet coherence of two time series x and y is:

$$\frac{|S(C_x^*(a,b)C_y(a,b))|^2}{S(|C_x(a,b)|^2)\cdot S(|C_y(a,b)|^2)}$$

where: Cx(a,b) and Cy(a,b) denote the continuous wavelet transforms of x and y at scales a and positions b.

For real-valued time series, the wavelet coherence is real-valued if you use a real-valued analysing wavelet, and complex-valued if you use a complex-valued analysing wavelet (TORRENCE C. and WEBSTER P. - 2016).

CASE STUDY AND RESULTS

We have extracted in Table 1, the 10 most important geomagnetic storms from 2022, according to https://www.spaceweatherlive.com/ and https://www.gfz-potsdam.de/en/, of which we analysed the first one with geomagnetic data according to https://intermagnet.github.io/, (BENOIT, 2012) for 6 observatories (4 from Europe – Spain, Germany, Greece and Romania; one from Canada and one from Antarctica) (Fig. 1).

Table 1. top 10 geomagnetic storms in 2022.

	TIME	Ap	00-03h	03-06h	06-09h	09-12h	12-15h	15-18h	18-21h	21-00h	Kp max
1	17/08/2022	32	1+	3	1	2+	2+	5-	7-	6-	7-
2	10/04/2022	29	2+	7-	5+	4-	2+	2	2	3-	7-
3	04/09/2022	62	5	6-	6	6+	5-	6	5-	5	6+
4	13/03/2022	40	1+	1-	0+	4	6-	5+	6-	6+	6+
5	14/04/2022	39	3+	3+	4	5-	4+	6	6-	4+	6
6	03/10/2022	24	4-	3	3	1+	4	4	6-	3	6-
7	26/12/2022	23	3-	2	3	4+	6-	5-	2-	1+	6-
8	07/08/2022	23	1	2	2+	3+	4	4	4	6-	6-
9	14/01/2022	15	0	0	0+	1	2	3-	4	6-	6-
10	14/03/2022	14	6-	3-	2-	2-	2-	2	1-	1	6-

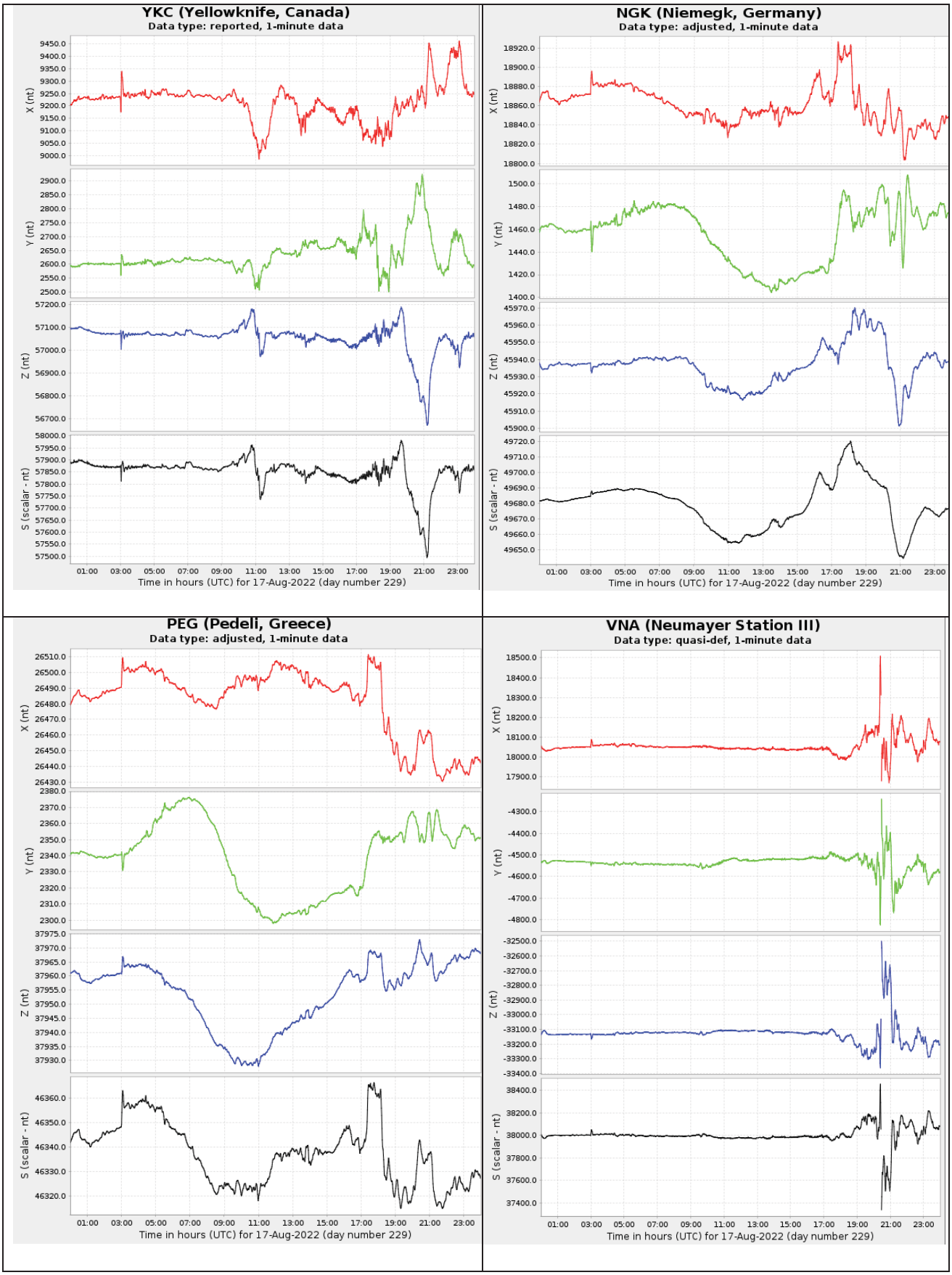

Figure 1. Magnetograms from 4 INTERMAGNET observatories (Yellowknife-Canada, Niemegk – Germany, Pedeli – Greece, Newmayer Station III – Antarctica) on August 17, 2022. In the images in figure 1 are the magnetograms with the notations from INTERMAGNET. Thus: X - North component, Y - East component, Z - vertical component, S - total component (scalar), nT or nt - nanoTesla (in the vertical axis of each image).

The *K-index* is a quasi-logarithmic local index of the 3-hourly range in magnetic activity relative to an assumed quiet-day curve for a single geomagnetic observatory site. The *K-index* consists of a single-digit 0 thru 9 for each 3-hour interval of the universal time day (UT).

The planetary 3-hour-range index *Kp* is the mean standardized *K-index* from 13 geomagnetic observatories between 44 degrees and 60 degrees northern or southern geomagnetic latitude. The scale is 0 to 9 expressed in thirds of a unit, e.g. 5- is 4 2/3, 5 is 5 and 5+ is 5 1/3. This planetary index is designed to measure solar particle radiation by its magnetic effects. The 3-hourly ap (equivalent range) index is derived from the *Kp index*.

The *Ap-index* provides a daily average level for geomagnetic activity. Because of the non-linear relationship of the *K-scale* to magnetometer fluctuations, it is not meaningful to take the average of a set of *K-indices*. Instead, every 3-hour *K-value* will be converted back into a linear scale called the a-index. The average from 8 daily a-values gives us the Ap-index of a certain day. The *Ap-index* is thus a geomagnetic activity index where days with high levels of geomagnetic activity have a higher daily *Ap-value*.

The *Ap*-index* is defined as the earliest occurring maximum 24-hour value obtained by computing an 8-point running average of successive 3-hour ap indices during a geomagnetic storm event and is uniquely associated with the storm event. The *AA*-index* is similar to the *Ap*-index*, but has a longer history and is based on reports from only two stations. (https://www.ngdc.noaa.gov/stp/geomag/kp_ap.html , https://www.spaceweatherlive.com/).

Figure 1 shows the variations of the tri-axial and total geomagnetic series for 4 observatories. The other two observatories (from Spain and Romania) were analysed in detail by wavelet analysis on each component (Figs. 2- 7).

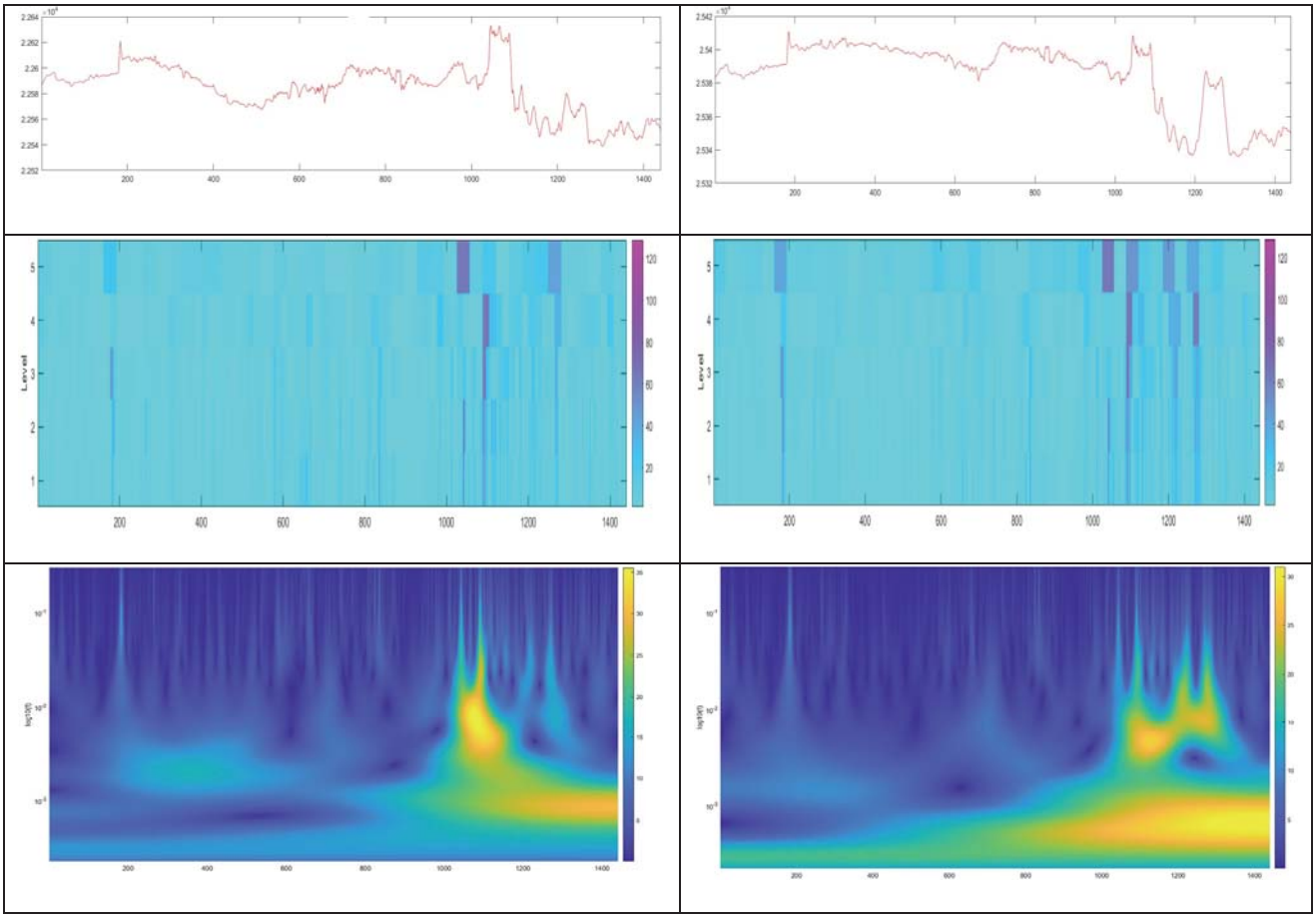

Figure 2. The geomagnetic component in the North direction (X) On the left side we find the data from the Surlari Observatory (Romania) and on the right side those from the Ebre Observatory (Spain). In the images above, the graphs of the recorded data are represented. The images in the centre show the absolute coefficients of the wavelet transform. In the images below are the wavelet analyses (on the abscissa is the time 1440 minutes from August 17, 2022; on the ordinate is the frequency; the legend on the right of the images shows the intensity - blue is minimum; yellow is maximum). In the graphs in the upper part of Fig. 2 the measurement units are nT (nanoTesla).

Wavelet Toolbox from Matlab (https://www.mathworks.com/) provides apps and functions for analysing and synthesizing signals and images. In figures 3 - 7 we can detect events like anomalies, change points, and transients, and denoise and compress data. Wavelet and other multiscale techniques can be used to analyse data at different time and frequency resolutions and to decompose signals and images into their various components. We can use wavelet techniques to reduce dimensionality and extract discriminating features from signals and images to train machine and deep learning models.

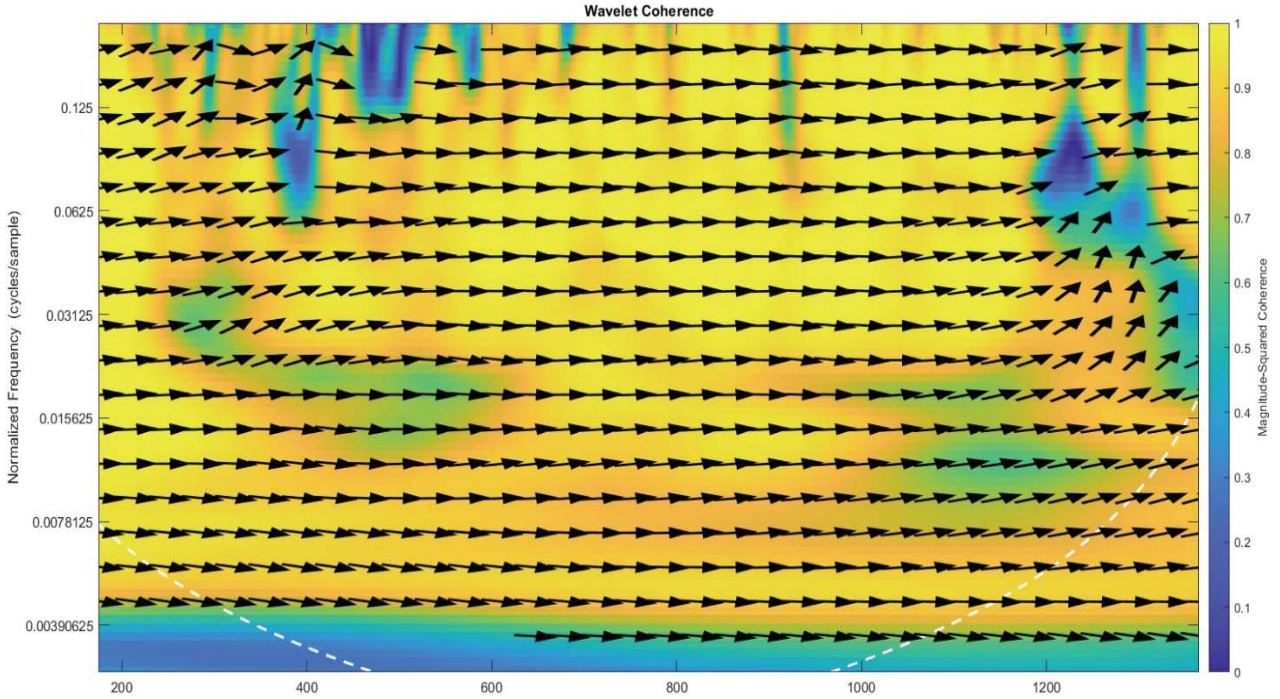

Figure 3. Wavelet coherence in the North (X) direction between the data recorded at the Surlari Observatory (Romania) and the data registered at the Ebre Observatory (Spain) on August 17, 2022.

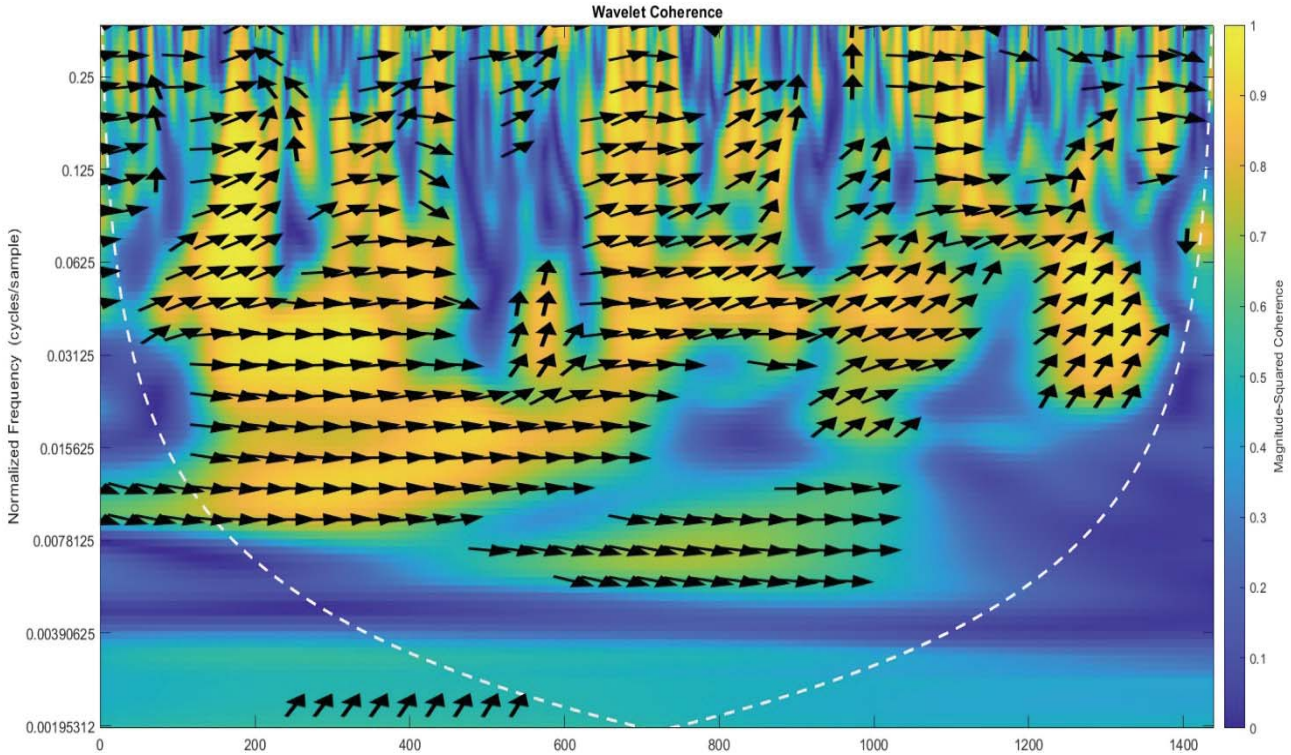

Figure 4. Wavelet coherence in the East (Y) direction between the data recorded at the Surlari Observatory (Romania) and the data registered at the Ebre Observatory (Spain) on August 17, 2022.

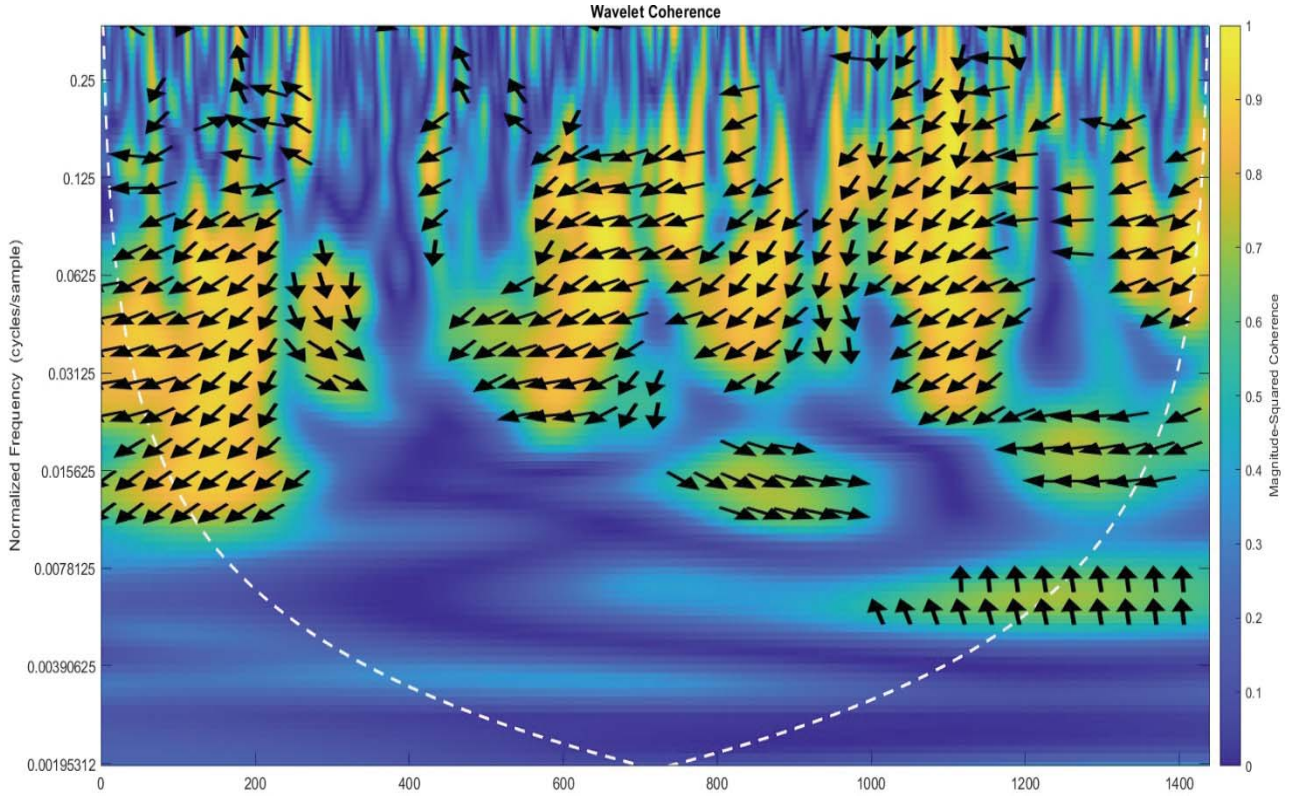

Figure 5. Wavelet coherence of the vertical geomagnetic field (Z) between the data recorded at the Surlari Observatory (Romania) and the data registered at the Ebre Observatory (Spain) on August 17, 2022.

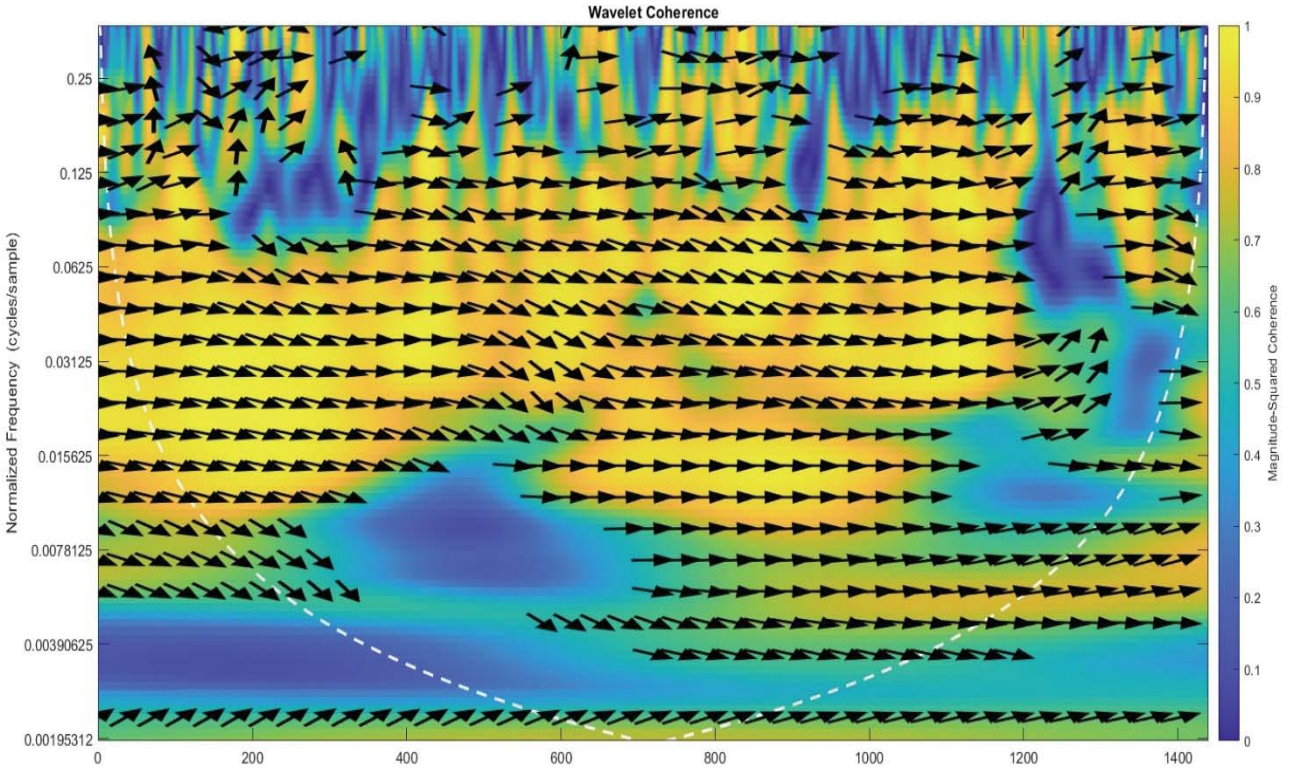

Figure 6. Wavelet coherence of the total geomagnetic field (F) between the data recorded at the Surlari Observatory (Romania) and the data registered at the Ebre Observatory (Spain) on August 17, 2022.

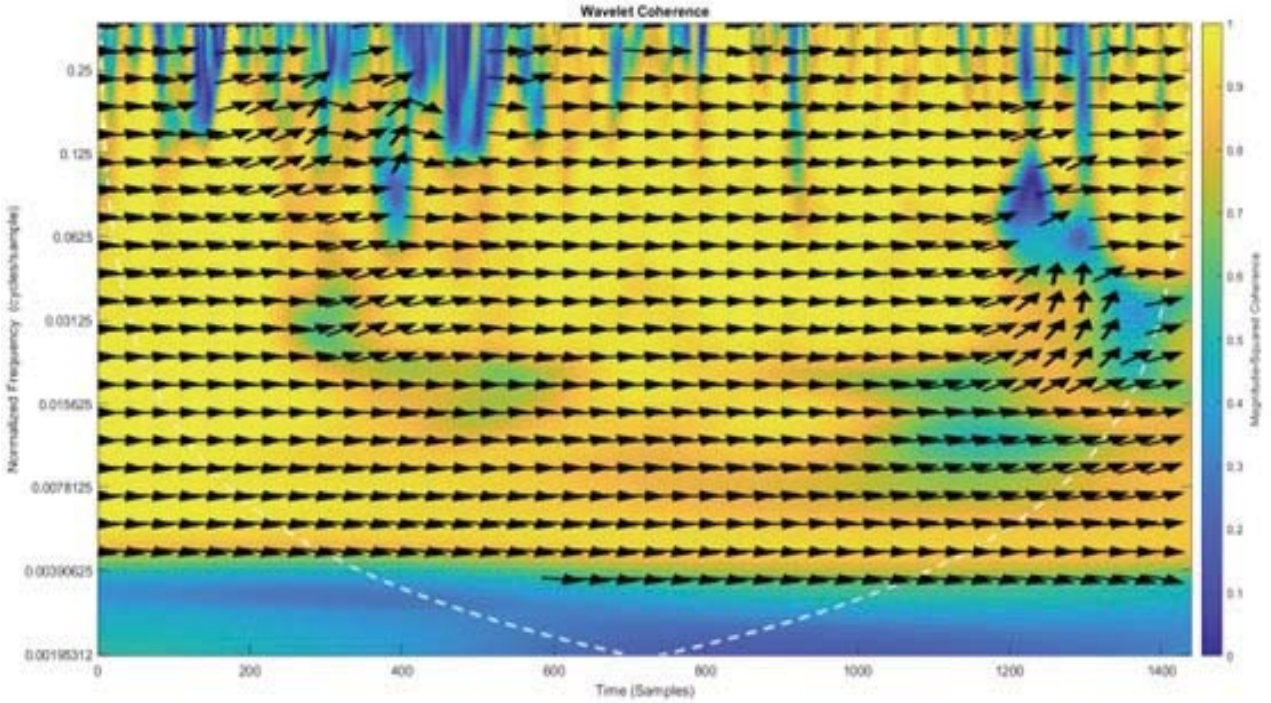

Figure 7. Wavelet coherence of the horizontal geomagnetic field (H) between the data recorded at the Surlari Observatory (Romania) and the data registered at the Ebre Observatory (Spain) on August 17, 2022.

A very good wavelet correlation can be noted for the north components (Fig. 3) and the horizontal components (Fig. 7) of the two observatories.

These two components are most affected by geomagnetic storms.

CONCLUSIONS

A first step in wavelet analysis is the short-time Fourier transform, applied successively with different narrow windows, for best time location accuracy. Increasing the window improves the resolution in frequency, but decreases its time resolution. We used CWT, beginning with adaptive time-frequency analysis using nonstationary Gabor frames, to analyse how the frequency content of a geomagnetic signal changes over time. For two signals, wavelet coherence reveals common time-varying patterns. Also, we can perform data-adaptive time-frequency analysis of nonlinear and nonstationary processes. Wavelet coherence, as a measure of the correlation between signals x and y in the time-frequency plane, was very useful for analysing nonstationary signals. The inputs geomagnetic time series, x and y, were with equal length, 1-D, real-valued signals. The coherence was computed using the analytical Morlet wavelet. Wavelet coherence returns the wavelet cross-spectrum of x and y. We used the phase of the wavelet cross-spectrum values to identify the relative lag between the input signals. Due to the inverse relationship between frequency and period, a plot that uses the sampling interval is the inverse of a plot that uses the sampling frequency. For areas where the coherence exceeds 0.5, plots that use the sampling frequency display arrows to show the phase lag of y with respect to x. The arrows are spaced in time and scale. The direction of the arrows corresponds to the phase lag on the unit circle. For example, a vertical arrow indicates a $\pi/2$ or quarter-cycle phase lag. The corresponding lag in time depends on the duration of the cycle.

Wavelet analysis, used for geomagnetic data from observatories, gives us information in the form of a three-dimensional graph (time, frequency, amplitude). In the two-dimensional plane, time and frequency are present and the amplitude is coded by colour intensity levels. This indicates with great accuracy the characteristics and time of occurrence of geomagnetic disturbances. From the comparisons made of the geomagnetic data analysed and exemplified we can observe a very good correlation between them during the analysed geomagnetic storm. In periods without magnetic disturbances, this correlation is no longer preserved.

From here, results the planetary character of the geomagnetic storms, varying only the amplitude of the disturbances.

ACKNOWLEDGEMENT

We thank to the IOSIN Surlari Geomagnetic Observatory and the INTERMAGNET Network for providing access to geomagnetic data. Also, we thank the Ministry of Research, Innovation and Digitalization for financing project from the Core Program PN23390401.

REFERENCES

ASIMOPOLOS N. S. & ASIMOPOLOS L. 2018. Study on the high-intensity geomagnetic storm from march 2015, based on terrestrial and satellite data. *Conference Paper of 18th International Multidisciplinary Scientific GeoConference SGEM 2018, Albena (Bulgaria), section Micro and Nano Tehnologies & Space Technologies & Planetary* Science. University Press. Sofia. **6**(1): 593-600.

ASIMOPOLOS L., SĂNDULESCU A. M., ASIMOPOLOS N. S., NICULICI E. 2012. *Analysis of data from Surlari National Geomagnetic Observatory*. Edit. Ars Docendi. București. 96 pp.

BOX G. E. P., JENKINS G. M., REINSEL G. C., LJUNG G. M. 2016. *Time series analysis - Forecasting and Control*. Fifth Edition. John Wiley & Sons. Hoboken. 709 pp.

BENOIT S. L. 2012. *INTERMAGNET Technical reference manual - Version 4.6*. Murchison House West Mains Road. Edinburgh. 100 pp.

CAMPBELL W. H. 2003. *Introduction to Geomagnetic Fields*. Cambridge University Press. London. 350 pp.

CONYERS L. B. 2016. *Ground-penetrating radar for geoarchaeology*. Wiley-Blackwell Publishers. London. 147 pp.

GRINSTED A. J., MOORE C., JEVREJEVA S. 2004. Application of the cross wavelet transform and wavelet coherence to geophysical time series. *Nonlinear Processes in Geophysics*. European Geosciens Union. München**. 11**(5-6): 561-566.

MARAUN D., KURTHS J., HOLSCHNEIDER M. 2007. Nonstationary Gaussian processes in wavelet domain: Synthesis, estimation and significance testing. *Physical Review*. American Physical Society. **75**: 1-14.

TORRENCE C. & WEBSTER P. 2016. Interdecadal changes in the ESNO-Monsoon System. *Journal of Climate. Colorado Boulder University*. **12**: 2679-2690.

***. https://www.spaceweatherlive.com/ (accessed: January 22, 2023).

***. https://www.gfz-potsdam.de/en/ (accessed: January 23, 2023).

***. https://intermagnet.github.io/ (accessed: January 24, 2023).

***. https://www.mathworks.com/ (accessed: January 24, 2023).

***. https://www.ngdc.noaa.gov/stp/geomag/kp_ap.html (accessed: January 26, 2023).

Asimopolos Laurențiu
Geological Institute of Romania
1st Caransebeş Street, 012271 - Bucharest, Romania.
E-mail: laurentiu.asimopolos@igr.ro, asimopolos@gmail.com

Asimopolos Natalia-Silvia
Geological Institute of Romania
1st Caransebeş Street, 012271 - Bucharest, Romania.
E-mail: natalia.asimopolos@igr.ro, asi_nata@yahoo.com

Asimopolos Adrian-Aristide
University POLITEHNICA of Bucharest, Faculty of Transports
313th Splaiul Independentei Street, 060042-Bucharest, Romania

Balea-Roman Bogdan-Valeriu-Constantin
Geological Institute of Romania
1st Caransebeş Street, 012271 - Bucharest, Romania.
E-mail: baleavaleriu@gmail.com

Received: March 22, 2023
Accepted: August 13, 2023